

## Effects of the solar wind electric field and ionospheric conductance on the cross polar cap potential: Results of global MHD modeling

V. G. Merkine,<sup>1</sup> K. Papadopoulos,<sup>1,2</sup> G. Milikh,<sup>2</sup> A. S. Sharma,<sup>2</sup> X. Shao,<sup>3</sup> J. Lyon,<sup>4</sup> and C. Goodrich<sup>5</sup>

Received 5 June 2003; revised 27 October 2003; accepted 30 October 2003; published 2 December 2003.

[1] The behavior of the cross polar cap potential,  $\Phi_{PC}$ , under strong solar wind conditions is studied using global MHD simulations. Simulations using two typical values of the ionospheric Pedersen conductance in agreement with others show that the cross polar cap potential is reduced compared to the corresponding potential in the solar wind due to the stagnation of the magnetosheath flow and the existence of parallel potentials. However, it is the ionospheric conductance that affects the value of  $\Phi_{PC}$  the most: the transpolar potential saturates only for high enough ionospheric conductance. A mechanism in which the ionospheric conductance changes the properties of the magnetosheath flow is proposed. This mechanism assumes mapping of the electrostatic potential in the ideal MHD system and yields a self-consistent response of the reconnection and transpolar potentials to changes in the ionospheric conductance. *INDEX TERMS*: 2736

Magnetospheric Physics: Magnetosphere/ionosphere interactions; 2753 Magnetospheric Physics: Numerical modeling; 2776 Magnetospheric Physics: Polar cap phenomena; 2784 Magnetospheric Physics: Solar wind/magnetosphere interactions. **Citation**: Merkine, V. G., K. Papadopoulos, G. Milikh, A. S. Sharma, X. Shao, J. Lyon, and C. Goodrich, Effects of the solar wind electric field and ionospheric conductance on the cross polar cap potential: Results of global MHD modeling, *Geophys. Res. Lett.*, 30(23), 2180, doi:10.1029/2003GL017903, 2003.

### 1. Introduction

[2] The cross polar cap or transpolar potential plays a key role in the solar wind-magnetosphere-ionosphere (SW-M-I) coupling. This potential,  $\Phi_{PC}$ , is the difference between the extrema of the electrostatic potential in the high-latitude ionosphere. Since electric fields are mapped onto the ionosphere along the magnetic field lines from the magnetopause and magnetotail, the transpolar potential is an important indicator of the coupling among the chain of events from the solar wind to the ionosphere.

[3] Recent observations indicate that the cross polar cap potential saturates when the convective electric field in the

solar wind,  $E_y$ , exceeds  $\sim 5$  mV/m level (for southward interplanetary magnetic field (IMF)) [Russell *et al.*, 2001; Hairston *et al.*, 2003]. For moderate solar wind activity  $\Phi_{PC}$  scales linearly with the solar wind convective electric field. However, for stronger solar wind  $E_y$ ,  $\Phi_{PC}$  shows almost no dependence on the solar wind conditions. The mechanisms for this effect are not fully understood at present. The recent model of the transpolar potential saturation [Siscoe *et al.*, 2002a] is based on the Hill model [Hill *et al.*, 1976; Hill, 1984] of magnetospheric convection and the role of the ionospheric conductance. In this model the saturation of the cross polar cap potential is attributed to the feedback from the region 1 current that limits the reconnection rate at the dayside magnetopause. In addition, Siscoe *et al.* [2002b] suggested a paradigm of a previously unrecognized storm-time magnetosphere in which the region 1 current rather than the Chapman-Ferraro current is dominant on the dayside magnetopause. In this model it is the region 1 current that balances the solar wind ram pressure and thus it cannot exceed the level required to resist the solar wind. Global MHD simulations by Raeder *et al.* [2001] indicate that there is a significant change in the shape of the magnetosphere under strong solar wind conditions: the lobes swell outwards shading the reconnection region, thus preventing the flow from reaching it. As pointed out by Siscoe *et al.* [2002a], these simulation results are in fact strongly interlinked because it is the current reconfiguration that leads to the change in the magnetopause geometry.

[4] Global MHD simulations are a natural tool to study  $\Phi_{PC}$  saturation. Despite the lack of reconnection physics underlying the SW-M-I interaction these simulations can reproduce many global phenomena of the system and its geometry. The saturation of the cross polar cap potential is in many respects a matter of geometry: the magnetopause is an obstacle in the way of the solar wind and changes in the geometry of the obstacle will naturally influence the properties of the flow around it.

[5] In this paper we present results of global MHD simulations of the SW-M-I system to study the transpolar potential under various solar wind conditions. The emphasis here is on the effect of the ionospheric conductance on the saturation level of the transpolar potential. A mechanism by which the ionospheric conductance can regulate the efficiency of the coupling in the system is presented.

### 2. Global MHD Simulations

[6] The Lyon-Fedder-Mobarry (LFM) global MHD code [e.g., Fedder and Lyon, 1995] is used to study the behavior of the cross polar cap potential under strong solar wind conditions. The latter were idealized: the velocity had only a

<sup>1</sup>Department of Physics, University of Maryland, College Park, Maryland, USA.

<sup>2</sup>Department of Astronomy, University of Maryland, College Park, Maryland, USA.

<sup>3</sup>NASA Goddard Space Flight Center, Greenbelt, Maryland, USA.

<sup>4</sup>Department of Physics and Astronomy, Dartmouth College, Hanover, New Hampshire, USA.

<sup>5</sup>Department of Astronomy, Boston University, Boston, Massachusetts, USA.

**Table 1.** The Solar Wind Parameters Used in the Simulations

Run #	1	2	3	4	5	6	7
$B_z$ , nT	-10	-15	-20	-25	-30	-35	-40
$V_x$ , km/s	-400	-400	-400	-400	-400	-400	-400
$n$ , $\text{cm}^{-3}$	5	5	5	15	20	25	30
$E_y$ , mV/m	4	6	8	10	12	14	16
$M_{ms}$	3.81	2.65	2.02	2.73	2.64	2.53	2.43

horizontal component which was kept constant throughout the runs and equal to 400 km/s and the magnetic field was purely southward with values from  $-10$  nT to  $-40$  nT. These conditions correspond to a solar wind convective electric field,  $E_y$ , in the range from 4 to 16 mV/m. It should be noted that the position of the bow shock depends strongly on the magnetosonic Mach number,  $M_{ms}$ , of the solar wind flow and for low enough  $M_{ms}$  (lower than 2 for this code) one can find the bow shock well outside the boundary of the grid located at about  $x_{GSM} = 24 R_E$ . Since  $M_{ms}$  reduces when the magnetic field is increased we had to alter the density so that  $M_{ms}$  was above 2. The solar wind parameters used in the runs are listed in Table 1.

[7] To examine the dependence of the cross polar cap potential on the ionospheric conductance and to facilitate the interpretation of the results the conductance was taken as a uniform Pedersen conductance,  $\Sigma_P$ . All runs were repeated for two values of  $\Sigma_P$  equal to 5 and 10 mhos. The constant solar wind conditions were held long enough (typically 5 hours) so that the system evolved into a steady state and the typical two-cell convection pattern was formed in the ionosphere. The results presented here correspond to a typical instant during the steady state.

### 2.1. Cross Polar Cap Potential and Reconnection Potential

[8] In the ideal MHD model and under steady state solar wind conditions the electrostatic potential is projected from the dayside magnetopause and from the magnetotail onto the polar ionosphere almost completely. The presence of non-ideal effects results in a relatively small potential attenuation due to the development of parallel electric fields along the magnetic field lines. Thus, the values of  $\Phi_{PC}$  and the reconnection potential are strongly related, and the two should be studied together. In a global MHD code the determination of physical quantities at the magnetopause is complicated due to the problem of locating the magnetopause, the absence of reconnection physics, and contamination with numerical noise. These difficulties are overcome, at least in part, by using the following technique. The extrema of the electrostatic potential are located inside the convection cells in the polar ionosphere. These points are on the boundary separating regions of open and closed magnetic field lines, and thus the field lines originating there connect to the ends of the reconnection line on the dayside magnetopause. The idea is to trace these field lines from their ionospheric footprints to the solar wind and to integrate parallel electric field along them. Then, taking the difference between two corresponding points on the field lines the potential drop between them can be computed. It should be noted that the parallel electric fields in the ideal MHD code are of numerical nature and therefore the specific magnitudes of the parallel electric fields obtained from the code may not be interpreted directly in terms of physical processes.

[9] Since the above procedure is subject to noise in the simulation data as well as the integration error, the footprints of the field lines should be determined carefully to make them pass as close as possible to the ends of the reconnection line. In Figure 1  $\Phi_{PC}$  and the reconnection potential calculated using this procedure are shown as functions of  $E_y$  for the two values of the ionospheric conductance used in the simulations. Evidently, the differences between the two corresponding curves are due to the parallel potential drop. It should be noted that in Figure 1 the potential difference between the solid and dashed lines for a given value of  $\Sigma_P$  is the difference between points on the two magnetic field lines. Therefore, the actual parallel potential drop along one field line is half the value in the figure. Let's consider the case with the largest parallel potential drop shown in Figure 1:  $E_y = 16$  mV/m and  $\Sigma_P = 5$  mhos. For this case the difference between the solid and dashed line is equal to 180 kV, and thus the actual parallel potential drop along one field line is 90 kV. Further, the parallel electric field along the field lines,  $E_{\parallel}$  is integrated up to the very end of the field line (where it reaches the boundary of the code grid) because of the problem of locating the intersection of the field line with the magnetopause.  $E_{\parallel}$  is naturally much higher inside of the magnetopause than outside of it. Moreover, beyond the bow shock  $E_{\parallel}$  becomes negligible in comparison with the total value of the electric field, but if the integration is continued over a long distance it still may give rise to a considerable potential drop as a result of accumulated numerical errors. Consequently, for the case discussed here this procedure yields a parallel potential which is about 30–40 kV higher than the potential difference between the point where the field line touches the reconnection line and its ionospheric footprint. The potential drop up to the magnetopause is about 50–60 kV, making the total parallel potential drop of about 90 kV. The solid lines depicted in Figure 1 represent overestimates of the reconnection potential and the actual value should be between the corresponding solid and dashed lines.

[10] Figure 1 shows the saturation of the transpolar potential as well as of the reconnection potential as  $E_y$  increases. The saturation of the reconnection potential is discussed in the following subsection. The other important feature of Figure 1 is the significant difference between the values of  $\Phi_{PC}$  and the corresponding reconnection potentials for different values of the ionospheric conductance. The saturation value of  $\Phi_{PC}$  at  $\Sigma_P = 5$  mhos is unrealisti-

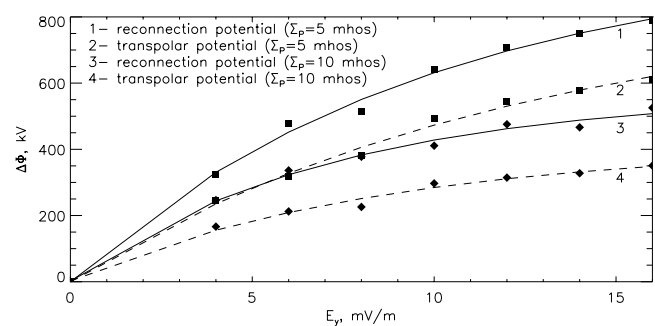


**Figure 1.** The cross polar cap and reconnection potentials,  $\Delta\Phi$ , as functions of the solar wind convective electric field,  $E_y$ . The lines are fits to the simulation data.

cally high as compared with the experimentally observed magnitudes [Russell *et al.*, 2001; Hairston *et al.*, 2003]. However, for  $\Sigma_P = 10$  mhos the situation improves: the level of  $\Phi_{PC} = 300$  kV at rather high solar wind convective electric field is much closer to the observations. The fact that the ionospheric conductance affects the value of the reconnection potential implies its influence on the properties of the magnetosheath flow. This is discussed in Subsection 2.3.

## 2.2. Magnetosheath Flow Stagnation and Saturation of the Reconnection Potential

[11] As we have seen in the previous section  $\Phi_{PC}$  saturates in a manner similar to the reconnection potential, given by the reconnection electric field and the length of the reconnection line. The reconnection electric field, in turn, is determined by the properties of the magnetosheath flow. In a hydrodynamic flow past an obstacle there is always a stagnation region where the velocity component transverse to the direction of the flow grows while the parallel component is reduced. In an MHD flow, the situation is similar to the hydrodynamic case, but the frozen-in magnetic field gets compressed so that the change in the convective electric field  $\vec{E} = -\vec{v} \times \vec{B}$  is expected to be smaller. This is examined using the simulation for the case with the solar wind  $B_z = -40$  nT and  $v_x = -400$  km/s ( $E_y = 16$  mV/m), and  $\Sigma_P = 10$  mhos. In this case the magnetic field at the nose of the magnetopause is compressed by a factor of  $\sim 3.1$  while the velocity is reduced by a factor  $\sim 7.7$  from the upstream values. This leads to a reduction of the convective electric field by more than 50%. Note that the change of the electric field across the bow shock can be neglected since the tangential component of the field must be conserved. The shock surface is quasi-perpendicular to the solar wind flow in a large region around the symmetry axis so that the electric field is mostly tangential to the shock and does not differ considerably on the two sides of the shock. Attenuation of this electric field in the magnetosheath leads to the reduction of the reconnection potential.

[12] The full magnetospheric potential taken as the product of the solar wind electric field and the characteristic size of the magnetosphere will correspond to a line that is above all the curves in Figure 1. This is due to the stagnation of the flow in the magnetosheath. However, the specific shape of the curves requires a more detailed analysis. The Hill model [Siscoe *et al.*, 2002a] provides a functional form of the transpolar potential dependence on the solar wind electric field and dynamic pressure. Further, Siscoe *et al.* [2002b] suggested that the amount of the region 1 current is limited by the solar wind dynamic pressure under extremely disturbed solar wind conditions, thus causing the saturation of the transpolar potential. It should be emphasized here that irrespective of the saturation mechanism, it should affect the global geometry of the system, and therefore, the magnetosheath flow so that the reconnection potential takes values consistent with the values of the transpolar potential. This should be true if the assumption about the mapping of electrostatic potential is valid, as expected in the ideal MHD model under steady state conditions.

## 2.3. Effect of the Ionospheric Conductance

[13] The global MHD simulations show that the reconnection and transpolar potentials saturate as the solar wind

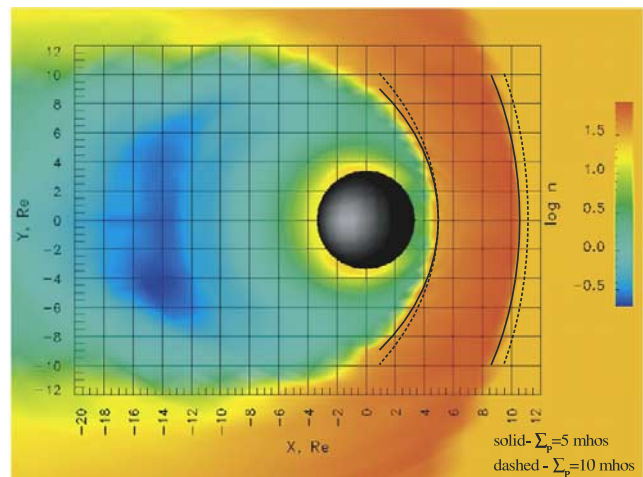


**Figure 2.** The magnetopause and the bow shock for the run #7. The background is the plasma density on a logarithmic scale for  $\Sigma_P = 5$  mhos. The curves are of the form  $r = \kappa/(1 + \epsilon \cos \theta)$  where  $\kappa$  and  $\epsilon$  are found from subsolar and terminator distances determined by the density jump.

electric field increases, as shown in Figure 1. However, the saturation level depends strongly on the ionospheric conductance. We have discussed above the reduction in the cross polar cap potential arising from the stagnation of the magnetosheath flow upstream of the magnetopause. We now address the question of how the ionosphere affects the properties of the magnetosheath flow.

[14] The role of the ionosphere in controlling magnetospheric convection as seen in global MHD simulations was first addressed by Fedder and Lyon [1987]. They discussed two distinct ways for such a control. First, it controls the length of the reconnection line, thus regulating the total amount of energy supplied to the ionosphere from the solar wind dynamo. Second, by regulating the strength of the region 1 currents, it influences the size of the region in the polar ionosphere through which open polar magnetic flux passes into the magnetosheath.

[15] The ionospheric control of the SW-M-I coupling is shown in Figure 2. In this figure the magnetosphere in the GSM XY plane is shown with the locations of the magnetopause and the bow shock for  $\Sigma_P = 5$  mhos (solid lines) and  $\Sigma_P = 10$  mhos (dashed lines). The background is the plasma density for  $\Sigma_P = 5$  mhos. The solar wind  $E_y = 16$  mV/m is the largest value used in the simulations. From Figure 2 it is easily seen that for the higher ionospheric conductance the magnetopause becomes wider at the flanks while the subsolar point distance does not change. This is a consequence of the increase of the region 1 currents and the resulting change in the location of the magnetopause across which pressure balance is achieved [Siscoe *et al.*, 2002b]. However, the constancy of the magnetopause subsolar point distance in the simulations may follow from the fact that the field aligned currents do not pass close to the nose of the magnetopause and thus do not contribute to the pressure balance there.

[16] The widening of the magnetopause is accompanied by an increase in the bow shock stand off distance, as seen

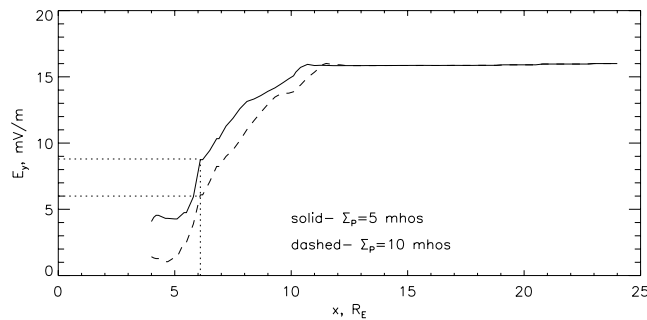


**Figure 3.** Profiles of  $E_y$  along the GSM  $x$ -axis in the magnetosheath for the run #7. The vertical dotted line represents the location of the point moved about  $1 R_E$  toward the Sun from the magnetopause subsolar point as determined from the density jump (see Figure 2). This is to make sure that numerical errors arising from the solution inside of the reconnection region are not included in the calculation.

in Figure 2. This is consistent with the results of *Farris and Russell* [1998].

[17] The displacement of the bow shock toward the Sun while the magnetopause subsolar point distance has not changed, leads to a wider magnetosheath. This means that the flow has more space to brake, and the solar wind convective electric field is expected to be smaller on the nose of the magnetopause. In Figure 3 we present the profiles of  $E_y$  along the GSM  $x$ -axis from 4 to  $24 R_E$ . From this figure we estimate that the difference between  $E_y$  at the nose of the magnetopause for the two conductances is about 3 mV/m. Assuming a reconnection line length of  $17 R_E$  for  $\Sigma_P = 5$  mhos and  $20 R_E$  for  $\Sigma_P = 10$  mhos (which corresponds to the simulations) we get a difference in the reconnection potential of about 200 kV. A potential difference of the same order of magnitude is seen in Figure 1. Thus, a slight shift of the bow shock toward the Sun by about  $1 R_E$  leads to a significant additional drop in the reconnection potential and consequently in the cross polar cap potential. The space scales of the system are so large that even small variations of the electric field result in appreciable potential drops.

### 3. Discussion and Conclusions

[18] Global MHD simulations have been used to study the behavior of the steady state cross polar cap potential under solar wind electric fields in the range 4 to 16 mV/m and two values of the ionospheric conductance ( $\Sigma_P = 5$  and 10 mhos). The simulations show that  $\Phi_{PC}$  saturates as  $E_y$  is increased, and the saturation level is strongly affected by the ionospheric conductance.

[19] The reconnection potential at the magnetopause, which is mapped to the polar ionosphere along equipotential magnetic field lines, is determined by the properties of the flow in the magnetosheath. Thus, independent of the physical mechanism that regulates the cross polar cap potential [*Siscoe et al.*, 2002a, 2002b] the geometry of the system and consequently the magnetosheath flow should change in a self-consistent manner. In this respect, the effect of the ionospheric conductance presented here becomes very

important. The simulations clearly indicate that under the same solar wind conditions the geometry of the magnetopause depends on the ionospheric conductance. For bigger conductances the magnetopause becomes wider at the flanks while preserving the subsolar point distance. This is a result of the increase of the region 1 currents and their possible sunward displacement on the surface of the magnetopause. The magnetopause widening leads to the bow shock shifting toward the Sun and a reduction of the convective electric field on the nose of the magnetopause. This, in turn, provides for smaller reconnection potential and consequently for smaller cross polar cap potential compared to the value at the smaller conductance.

[20] *Fedder and Lyon*, [1987] suggested that the SW-M-I system is self-regulating, so that an increasing power input from the solar wind to the polar ionosphere leads to an increase in the ionospheric conductance which reduces the coupling efficiency. The effect of the ionospheric conductance presented here is consistent with this picture and provides a mechanism by which the conductance can regulate the coupling of the solar wind to the magnetosphere and ionosphere.

[21] The recent work by *Siscoe et al.* [2002a, 2002b] implies that the transpolar potential saturates as  $E_y$  increases while the reconnection potential does not. The mechanism presented in this paper, on the other hand, is due to a self-consistent reconfiguration of the system in response to changes in the ionospheric conductance, assuming mapping of electrostatic potential. This leads to a saturation of both the reconnection potential and the transpolar potential. Further studies of the parallel potential drops near the magnetopause are needed to resolve the differences between these mechanisms.

[22] **Acknowledgments.** This research was supported by NASA grants NAG513452 and NAG510882, and NSF grant ATM0119196. The authors are grateful to T. Hill for helpful discussions. We thank NCSA for computational resources used to complete the simulations.

### References

- Farris, M. H., and C. T. Russell, Determining the standoff distance of the bow shock: Mach number dependence and use of models, *J. Geophys. Res.*, *99*(A9), 17,681–17,690, 1998.
- Fedder, J. A., and J. G. Lyon, The solar wind-magnetosphere-ionosphere current-voltage relationship, *Geophys. Res. Lett.*, *14*, 880–883, 1987.
- Fedder, J. A., and J. G. Lyon, The Earth's magnetosphere is  $165 R_E$  long: Self consistent currents, convection, magnetospheric structure, and processes for northward interplanetary magnetic field, *J. Geophys. Res.*, *100*(A3), 3623–3636, 1995.
- Hairston, M. R., T. W. Hill, and R. A. Heelis, Observed saturation of the ionospheric polar cap potential during the 31 March 2001 storm, *Geophys. Res. Lett.*, *30*(6), 1325, doi:10.1029/2002GL015894, 2003.
- Hill, T. W., Magnetic coupling between solar wind and magnetosphere: Regulated by ionospheric conductance?, *Eos Trans. AGU*, *65*, 1047–1048, 1984.
- Hill, T. W., A. J. Dessler, and R. A. Wolf, Mercury and Mars: The role of ionospheric conductivity in the acceleration of magnetospheric particles, *Geophys. Res. Lett.*, *3*, 429–432, 1976.
- Raeder, J., Y. Wang, and H. J. Singer, Global simulation of space weather effects of the Bastille Day storm, *Solar Physics*, *204*, 325, 2001.
- Russell, C. T., J. G. Luhmann, and G. Lu, Nonlinear response of the polar ionosphere to large values of the interplanetary electric field, *J. Geophys. Res.*, *106*, 18,495–18,504, 2001.
- Siscoe, G. L., G. M. Erickson, B. U. Ö. Sonnerup, N. C. Maynard, J. A. Schoendorf, K. D. Siebert, D. R. Weimer, W. W. White, and G. R. Wilson, Hill model of transpolar potential saturation: Comparisons with MHD simulations, *J. Geophys. Res.*, *107*(A6), 1075, doi:10.1029/2001JA000109, 2002a.
- Siscoe, G. L., N. U. Crooker, and K. D. Siebert, Transpolar potential saturation: Roles of region 1 current system and solar wind ram pres-

sure, *J. Geophys. Res.*, 107(A10), 1321, doi:10.1029/2001JA009176, 2002b.

---

V. G. Merkine and K. Papadopoulos, Department of Physics, University of Maryland, College Park, MD 20742, USA. (merkin@astro.umd.edu)

G. Milikh and A. S. Sharma, Department of Astronomy, University of Maryland, College Park, MD, USA.

X. Shao, NASA Goddard Space Flight Center, Greenbelt, MD, USA.

J. Lyon, Department of Physics and Astronomy, Dartmouth College, Hanover, NH, USA.

C. Goodrich, Department of Astronomy, Boston University, Boston, MA, USA.